An Electrochemical Pipette for the Study of Drug Metabolite

Nastaran Nikzad,[a] Buwanila T. Punchihewa,[a] Vidit Minda,[b] William G. Gutheil,[b] and Mohammad Rafiee*[a]

a. Division of Energy, Matter and Systems, School of Science and Engineering, University of Missouri-Kansas City, Kansas City, MO 64110 (USA)

b. Division of Pharmacology and Pharmaceutical Sciences, University of Missouri-Kansas City, Kansas City, MO 64108 (USA)

* Email: mrafiee@umkc.edu.

KEYWORDS: Drug metabolites, Thin-layer electrochemistry, Microelectrode, Electrolysis, Electroanalysis.

ABSTRACT: Electrochemistry offers an effective means of mimicking enzymatic metabolite pathways, particularly the oxidative pathways catalyzed by the cytochrome P450 superfamily. The electrochemical generation and identification of metabolites are time-sensitive, necessitating adjustable cell designs for accurate mechanistic interpretation. We present a thin-layer electrode (TLE) that addresses the needs of both analytical and synthetic electrochemical generation of drug metabolites. The TLE's ability to conduct experiments on a minute-to-hour timescale allows for detailed observation of reaction mechanisms for metabolites not easily identified by traditional methods. The utility of the TLE for drug metabolite was benchmarked for electrochemical oxidation of acetaminophen, acebutolol, and 2-acetyl-4-butyramidophenol, known to produce quinone imine metabolites, i.e., NAPQI, upon oxidation. When combined with a microelectrode (μE), the TLE enables probing the concentration profiles for metabolic oxidation of these drugs. The micromole scale and pipette-type structure of the TLE facilitate comprehensive structural elucidation of intermediates and products using chromatographic and spectroscopic techniques.

INTRODUCTION

The drug metabolism process involves a variety of chemical reactions, including oxidation, reduction, hydrolysis, and conjugation, to either activate or deactivate drug molecules, ultimately leading to their excretion from the body. The initial phase of xenobiotic elimination predominantly entails first-pass hepatic oxidation, occurring at the catalytic site of enzymes belonging to the Cytochrome p450 (CYP450) family.[1-6] Simulating hepatic oxidation is crucial for understanding major metabolic pathways and optimizing the drug discovery and development process.[7–9] In vitro, cytochrome P450 enzyme incubation is a well-known method for simulating and studying drug metabolites.[10-14] Electrochemistry, mainly due to its tunable electrode potential and mild reaction conditions, represents another promising approach for studying drug metabolites and promises to expedite this process efficiently.[15–17] Electrochemical techniques used for studying drug metabolites include electroanalytical and electrolysis techniques.[18] The timescale of electroanalytical techniques, such as cyclic voltammetry, ranges from microseconds to a few minutes,[19-22] making them suitable for generating and studying short-lived intermediates and/or products.[23] However, with a reaction scale limited to the diffusion layer and negligible compared to the solution bulk, isolating the electrode reaction product is not feasible (*Fig 1a*).[24-26] Bulk electrolysis reactions offer an extended timescale, typically more than an hour to overnight, with reaction scales suitable for the isolation and structural elucidation of drug metabolites (*Fig 1c*).[25] The timescale of the electrolysis reaction is determined by the mass transfer regime and the electrode surface area (A) to cell volume (V) ratio, making the electrolysis time unadjustable and prolonged, which affects the profile of time-sensitive products and intermediates.

We recently introduced a pipette-type thin-layer electrode (TLE) for rapid electrolysis reactions within the timeframe characteristic of electroanalytical techniques (*Fig 1b*).[27] The principle of thin-layer electrochemistry is confining a small solution volume within a thin layer comparable to the thickness of the diffusion layer at the electrode surface.[28-34]

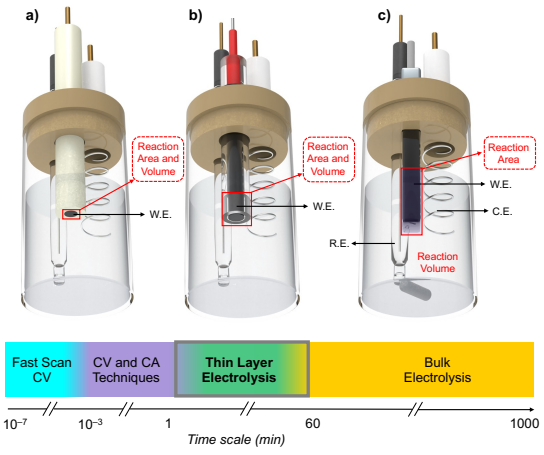

Fig. 1. Schematic presentation of reaction area of a) electroanalytical cell, b) thin layer electrode, c) electrolysis cell with the corresponding timescales for each cell.

This provides a substantial A/V improvement and the opportunity to overcome the limitations of conventional electrolysis cells. The electrolysis reaction in the TLE requires 2 to 20 minutes, and confining the solution in the TLE allows for adjusting the time needed to probe the reaction species over extended periods (*Fig 1*). A timescale that bridges the gap between the timescales of electroanalytical methods and typical electrolysis reactions. (Fig 1b) The pipette-type structure of the electrode and the solution volume of TLE aid in preparing the sample for further structural elucidation of the reaction products and intermediates.[35,36] Moreover, hosting a microelectrode (μE) in the TLE enables real-time probing of the redox events or their coupled chemical reactions during thin-layer electrolysis.[27,37] The details of TLE and μE fabrication and integration of μE into the TLE are described in the Supporting Information, Sections 1 to 3, and Figures S1 to S8. Herein, the utility of this pipette-type TLE for the study of the drug metabolites is benchmarked using the oxidation of acetaminophen (**1a**), acebutolol (**2a**), and its proximate metabolite 2-acetyl-4-butyramidophenol (**2d**). Oxidation of all these molecules leads to the formation of N-acetyl-p-benzoquinoneimine (NAPQI) metabolites, in which the harmful side effects of these drugs are attributed to their metabolic formation.[38-44]

RESULTS & DISCUSSION

Study of the metabolites under neutral conditions. We initiated our study using cyclic voltammetry on disk electrodes. Under mild acidic and neutral conditions, the cyclic voltammogram (CV) of acetaminophen showed an anodic peak (A_1) for oxidation of acetaminophen (**1a**) to N-acetyl-p-benzoquinone imine (**1b**), and a cathodic peak (C_1) corresponds to the reduction of electrochemically generated **1b**. A peak-to-peak separation greater than 60 mV that increases with scan rate, and a slight decay in the normalized peak current of A_1 with increasing scan rate, indicated a quasi-reversible redox behavior for **1a** (*Fig 2a*). The cathodic-to-anodic peak current ratio (C_1/A_1) remains the same at various scan rates, indicating the relative stability of the **1b** under mild acidic and neutral conditions (please see Fig S9 and S10 in Supporting Information).[39] The C_1/A_1 peak current ratio decays by extending the timescale of the voltammetric experiment at very low scan rates (i.e., 5 mVs^{-1}, please see Fig S10 in Supporting Information). However, such measurements may be inaccurate due to the build-up of density gradients and convective disruption of the diffusion layer.[28] By confining the solution within the TLE, it becomes feasible to conduct voltammetric experiments at very low scan rates, up to 0.2 mVs^{-1}, thereby extending the experiment's duration for probing the reactivity of electrochemically generated **1b**. CV of **1a** in TLE, at 1 mVs^{-1}, exhibited A_1 and C_1 peaks that are symmetrical about the peak potentials, and return to the baseline at the end of each half cycle, matching the bell-shaped characteristic CV of TLE (*Fig 2b*). The cathodic-to-anodic peak current ratio (I_{pC}/I_{pA}) was less than unity, indicating the instability of **1b** within the time scale of the voltammetric experiment in TLE. The amount of **1a** and **1b** for each half cycle can be determined by measuring the consumed charge, derived by current–time integration (dashed line in *Fig 2*), providing a quantitative means for measuring the reactivity. The ratio of the consumed charges for the cathodic and anodic reactions of voltammetry in TLE was 0.78, indicating consumption of >20% of **1b** within a 10-minute scale of this voltammetric experiment. It should be noted that a ratio of less than unity was not related to diffusive leakage from the TLE. No significant diffusive leak from the TLE was observed within the timescale of this experiment, and even up to 4 hours.[27] CV of acebutolol (**2a**), under similar conditions, showed an anodic peak (A_2 in *Fig 2c*) at more positive potentials, compared to **1a**, with no cathodic counterpart peak. A pair of new cathodic (C'_1) and anodic (A'_1) peaks appeared in the second and third half-cycles of CV, respectively. The lack of reduction peak for the CV of **2a** is due to the conversion of its oxidation product (**2b**) to a benzoquinone imine (N-(3-acetyl-4-oxocyclohexa-2,5-dienylidene)butyramide (**2c**) via a C–O bond cleavage.

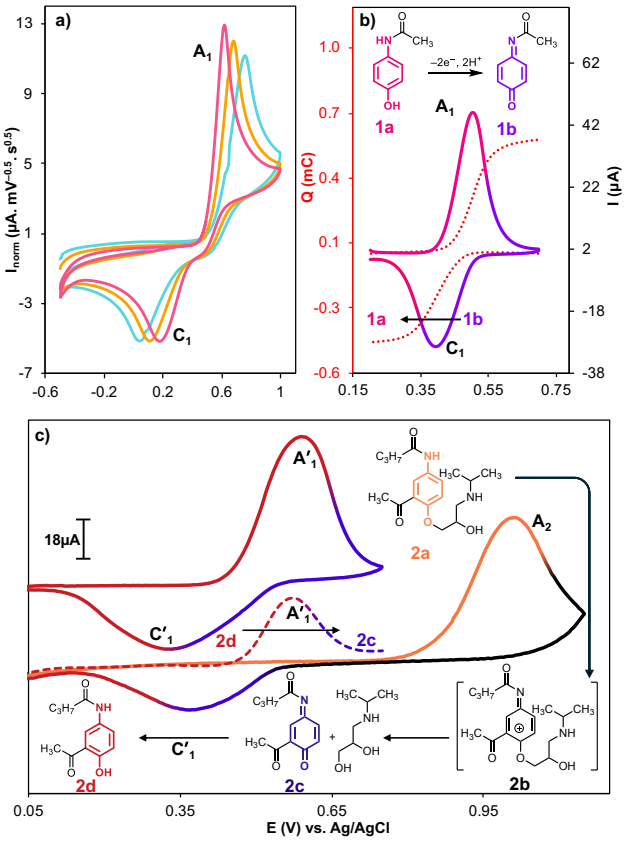

Fig. 2. a) Normalized CVs of **1a** on GC disk electrode at 20, 100, and 500 mVs^{-1}. b) CV of **1a** in TLE and the consumed charge in each half-cycle (dotted line). c) CVs of **2a** and **2d**, in TLE, third half-cycle for CV of **2a** is presented in dashed line. Reaction conditions: buffer solution of pH=6, 2 mM of each substrate, 1 mVs^{-1} scan rate for TLE experiments.

Compound **2c** can also be generated from direct oxidation of 2-acetyl-4-butyramidophenol (**2d**). The potentials and shapes of A'_1 and C'_1 precisely match the voltammetric features of **2d** (*Fig 2c*). The ratio of the consumed charges for the cathodic and anodic reactions of **2d** and **2c**, respectively, indicates that 30% of **2c** was consumed (please see Fig S11 in Supporting Information), and it is slightly less stable than **1b** (20% of **1b** was consumed in a similar experiment). Voltammetric studies of **1a** and **2d** using disk electrodes showed no noticeable reaction or difference between the stability of **1b** and **2c**. To extend the timescale of the experiment further, and probe the stability of **1b** and **2c**, the combination of TLE and microelectrode (μE) was used. Owing to the lack of diffusion limitations, μEs provide a means to assess the bulk concentration of electroactive species and their concentration during chemical reactions. This feature enables the investigation of short-lived intermediates

and the real-time monitoring of electrolysis reactions, which is hindered by the prolonged reaction times dictated by convection and the design of conventional cells. This TLE setup facilitates real-time monitoring of electrolysis reactions by eliminating semi-infinite mass transfer and confining the reaction chamber. *Fig 3* shows the fabricated TLE with an accommodated miniaturized µE. In this setup, electrolysis was performed on a glassy carbon (GC) rod, and µE served as a probing electrode. Linear sweep voltammogram (LSV) of **2d**, recorded by µE before electrolysis, exhibited a sigmoidal shape with a plateau current (A'_1, *Fig 3c*). By setting the potential of the GC rod at 0.7 V, measured from LSV recorded by µE, an electrolysis trace was obtained for oxidation of **2d**. The electrolysis current reached 2% of the initial current in 5 minutes of electrolysis time (*Fig 3d*) due to the consumption of **2d** in TLE. A recorded LSV, using µE, after electrolysis indicated quantitative conversion of **2d** to **2c** (*Fig 3c*) and formation of a reductive plateau current (C'_1, *Fig 3e*). The plateau currents of A'_1 and C'_1 are proportional to the concentrations of **2d** to **2c**, respectively, in TLE.

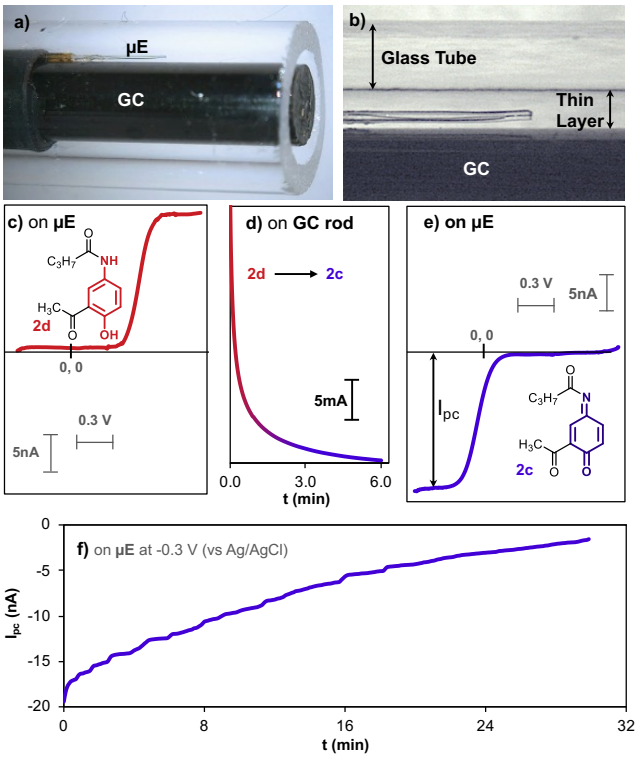

Fig. 3. a), b) Pictures of thin layer electrode with integrated microelectrode. c) LSV of **2d** recorded using microelectrode, d) electrolysis trace for conversion of **2d** to **2c** at 0.8 V in TLE, and e) LSV of electrochemically generated **2c** f) chronoamperogram of **2c** obtained by setting the potential of microelectrode at –0.3 V. Reaction conditions: buffer solution with pH 6, initial concentration of **2d** = 2 mM, scan rate for LSVs = 50 mV/s^{-1}.

A chronoamperometric experiment, performed by setting the potential of µE at the C'_1 plateau, allowed us to derive the concentration profile of **2c** over time (Fig. 3f). Analysis of this concentration profile indicates that the half-life of **2c** is 550 s, and the rate constant of its reaction is 1.3×10^{-3} s^{-1} (please see Section 5 in the SI and Figure S14 for more details). The half-life and rate constant for the reaction of **1b**, determined using a similar experiment, were 707 seconds and 9.8×10^{-4} s^{-1}. These data prove that the degradation rate of **1b** and **2c** can't be measured within the timescale of the voltammetric experiment. It also indicates that these quinone imine metabolites are not stable enough to be detected after electrolysis using traditional electrolysis cells. Performing LSV experiments during and at the end of two-hour electrolysis using a commercially available electrolysis cell showed accumulation of no more than 2% **1b** or **2c**.[45]

The experiment described here indicates that electrochemical and mass spectroscopic techniques can detect the reaction products for oxidation of **1a** to **1b** and **2a** or **2d** to **2c**. However, **1b** and **2c** are unstable for isolation and further structural elucidation. This finding aligns with numerous other drug metabolite studies, suggesting that the instability and toxicity of drug metabolites correlate with the reactivity of their oxidized forms.[46] To prevent the degradation of electrochemically generated metabolites, one approach is to reduce them to more stable forms, not necessarily the initial parent drug.[47] To test this approach, a double-step electrochemical technique was employed to synthesize **2d** from **2a**. The first step involved an anodic process converting **2a** to **2c** (*Fig 4a*), followed immediately by a reductive step resulting in the conversion of **2c** to the shelf-stable metabolite **2d** (*Figure 4a*).

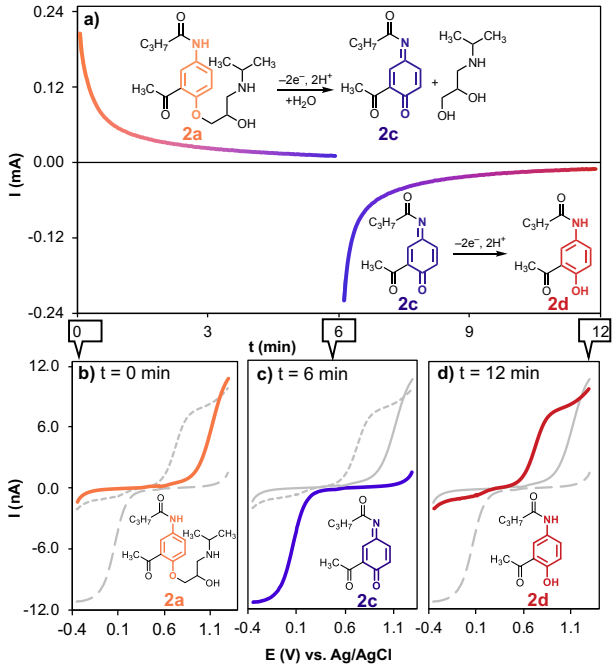

Fig. 4. a) double-step electrolysis reactions for oxidation of **2a** to **2c**, and reduction of electrochemically generated **2b** to **2c**. b) LSV of **2a** before oxidation, c) LSV of electrochemically generated **2c**, and d) LSV of electrochemically generated **2d**. LSVs recorded on microelectrode, and the gray LSVs are overlaid to show the stepwise reaction process. Reaction conditions: buffer solution with pH 6, 2 mM initial concentration of **2d**, scan rate for LSVs = 50 mVs^{-1}; the potentials for double-step electrolysis are 1.1 and –0.3 V (vs. Ag/AgCl), respectively.

The formation of **2c** and **2d** was confirmed by recording their LSV using µE (*Fig 4b* to *4d*) and by HPLC-MS analysis and the isolated yield for the resulting **2d** was 53% (please see sections 6 and 7 of Supplementary Information). Confining the solution in a thin layer makes a sequential approach possible, and a short electrolysis time prevents the side reaction and degradation of electrochemically generated intermediates.

Study of the metabolites under acidic conditions. Under acidic conditions, the oxidation peaks of **2a** (A_2) and **2d** (A'_1) shifted to more positive potentials due to coupled proton transfer reactions during their electrochemical processes (*Fig 5a* and *5b*). The C'_1 reduction peak disappeared due to the formation of an electroinactive adduct (**2e**) between water and protonated **2c**. **2e** subsequently undergoes the chemical transformation into the corresponding benzoquinone (**2f**) by dissociating the butyramide group (*Fig 5f*). Both cyclic voltammograms (CVs) obtained using the disk electrode and thin-layer electrode (TLE) for **2a** showed the absence of the C'_1 peak. However, only the TLE CV revealed the redox features of quinone/hydroquinone derivatives (C_3/A_3). The conversion of **2e** to **2f** occurs slowly, leading to negligible accumulation of **2f** near the electrode surface within the typical timescale of voltammetric experiments. CV of **2a** recorded by disk electrode showed only one anodic peak (*Fig 5d,* please also see Fig S12 in Supporting Information). In contrast, the extended timescale of TLE experiments not only captures the CV characteristics of **2e** (*Fig 5b*) but also detects subsequent chemical reactions, including Michael's addition of water to form **2g** (*Fig 5b and 5c*).

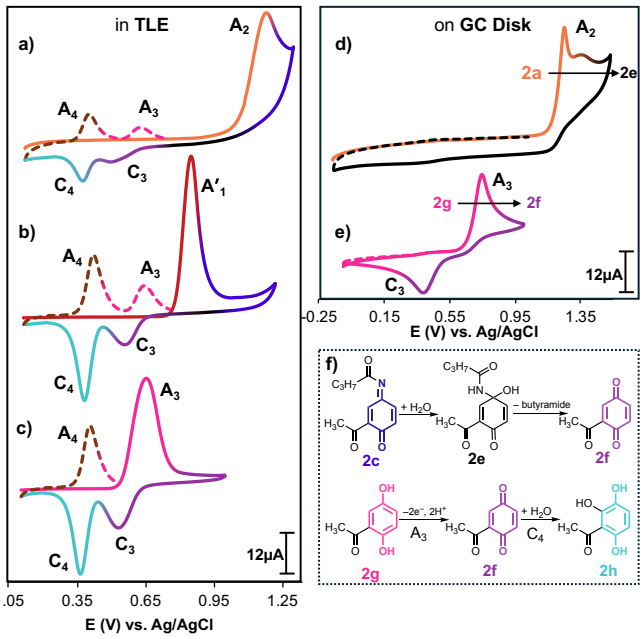

Fig. 5. a) to c) CVs **2a**, **2d**, and **2g** recorded in TLE compared to CVs **2a** and **2g** (curves d and e) on a GC disk electrode. f) the mechanisms of **2c** and **2g** oxidation under acidic conditions. Reaction conditions: 0.5 M perchloric acid solution, scan rate for voltammetric experiments in TLE is 1 mVs^{-1}, scan rate for voltammetric experiments on GC disk is 50 mVs^{-1}, initial concentration of all substrates is 2 mM.

Essentially, TLE allowed visualization of all chemical transformations involving **2e**, whereas such reactions were not observable within the shorter timescale of voltammetry at the disk electrode. Similar results were obtained for capturing the CV characteristics of the benzoquinone (**1d**) from the oxidation of acetaminophen (**1a**, please see Fig S13 in Supporting Information).

The results of the voltammetric studies revealed that the electrochemically generated quinoneimine (i.e., **1b**) undergoes a fast reaction with water followed by a slow elimination of the amide group. This results in the transient accumulation of electroinactive intermediate (i.e., **1c**) prior to the rate-limiting formation of corresponding benzoquinone (**1d**). A dual-electrochemical experiment was designed, utilizing the combined μE-TLE and a bipotentiostat to gain more insights into these consecutive reactions. The potential of GC in TLE was set at the oxidation potential of **1a**, and the μE's potential was scanned concomitantly in a linear sweep mode to obtain multi-LSV during electrolysis (*Fig 6*).[48]) The electrolysis current declined and reached the background current in 15 minutes due to the consumption of **1a**. The A_1 plateau current of LSV, corresponding to the **1a** oxidation, decreased during electrolysis. No reduction current was observed for **1b** due to its rapid consumption by the water addition reaction. A plateau, C_5, corresponding to the reduction of parabenzoquinone (**1d**), appeared with a 3-minute delay, and its current increased gradually over the course of the electrolysis reaction.

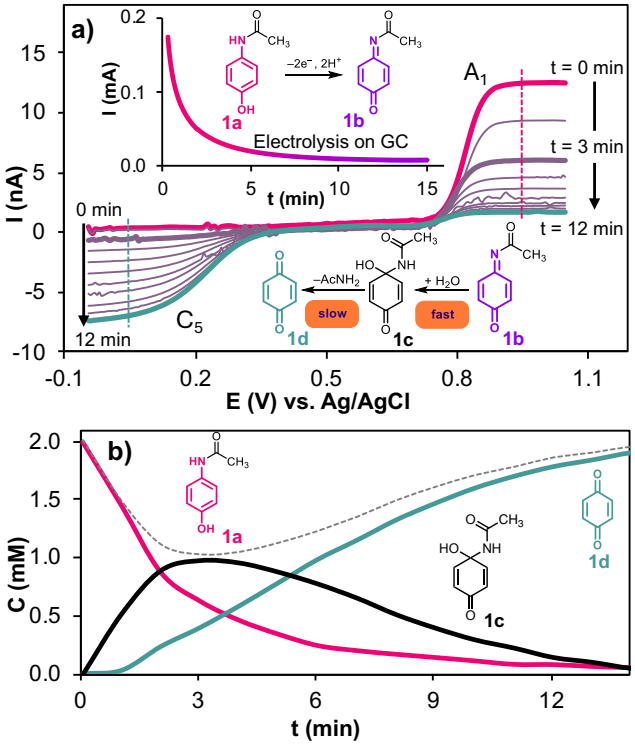

Fig. 6. a) multi-scan LSV (on microelectrode) during electrochemical oxidation of **1a** (in TLE) under acidic conditions, electrolysis trace is shown in the inset. b) derived concentration profile of reaction components during electrolysis. Reaction conditions: 0.5 M perchloric acid solution, initial concentration of **1a** is 2 mM, scan rate for LSV experiments = 50 mVs^{-1}, applied potential for electrolysis in TLE = 1.0 V vs Ag/AgCl.

The plateau currents of A_1 and C_5 are proportional to the concentrations of **1a** and **1d**, respectively. Sampling the positive and negative currents of multi-scan LSV and concentration-current calibration enabled the derivation of the concentration profiles of **1a** and **1d** during electrolysis. The potentials for current sampling are indicated with dashed lines in *Fig 6a*. The sum of **1a** and **1d** concentrations is less than the initial concentration of **1a**, due to the accumulation of electroinactive **1c** intermediate (dashed line in *Fig 6b*). Formation of an electro-inactive intermediate was also noticeable from the LSV plots, and the increase in the C_5 plateau current was not proportional to the decay in the A_1 current, especially at the beginning of the reaction. For example, after 3 minutes of electrolysis, the A_1 current decayed by more than 50%, whereas C_5 reached only 10% of its maximum. The dual electrolysis experiment proved the formation of an electro-inactive intermediate **1c**, where its

conversion to **1d** was the bottleneck of the reaction. The designed experimental setup also allowed derivation of the concentration profile of **1c** by subtracting the concentrations of **1a** and **1d** from the total concentration. The rate constant of the **1c** to **1d** reaction was derived by analyzing and fitting the concentration profiles; it equals 0.29 Ms^{-1}.

CONCLUSIONS

In conclusion, this study highlights the advantages of omitting inbound convective mass transfer in thin-layer electrodes (TLE) to achieve rapid electrolysis reactions within an adjustable timeframe. This method proves especially valuable for detecting intermediate and unstable products, such as drug metabolites, with half-lives ranging from minutes to an hour. The effectiveness of TLEs was demonstrated through the analysis of electrochemically generated quinone imines resulting from the oxidation of acebutolol, acetaminophen, and 2-acetyl-4-butyramidophenol. Using TLE to study quinone imines allowed us to detect intermediates and visualize the reactions involved in the metabolic processes of these compounds—features that conventional electroanalytical or electrosynthetic cells fail to reproduce. The pipette-type TLE designed in this study features several notable advantages: a) a sample size suitable for spectroscopic and chromatographic analysis, b) ease of sample loading and dispensing, c) an extended and adjustable experimental time scale, d) the ability to conduct synthetic double-step experiments, and e) the integration of a microelectrode for dual electrochemical experiments. Notably, the integration of a microelectrode allows for potential scanning during electrolysis, facilitating the visualization of concentration profiles for all reaction components throughout the process.

EXPERIMENTAL SECTION

Chemicals: Acetonitrile (CAS-75-05-8), Acetone (CAS-67-64-1), Sodium bicarbonate (CAS-144-55-8), Sodium carbonate (CAS-497-19-8), Sodium hydroxide (CAS-103-90-2), 2-Acetyl-4-butyramidophenol (also known as N-(3-acetyl-4-hydroxyphenyl)butyramide CAS-40188-45-2), Perchloric acid (CAS-7601-90-3), and Dimethyl sulfoxide (DMSO, CAS-67-68-5) were purchased from ThermoFisher Scientific. Acetaminophen (CAS-103-90-2), Acebutolol hydrochloride (CAS-34381-68-5), 2',5'-Dihydroxyacetophenone (CAS-490-78-8), and potassium hydrogen phthalate (CAS-877-24-7) were purchased from Sigma Aldrich. LC/MS grade water with 0.1% formic acid (CAS-7732-18-5, 64-18-6) and acetonitrile with 0.1% formic acid (CAS-75-05-8) were purchased from Fisher Scientific. All chemicals and solvents were purchased from commercially available sources and used without further purification.

Material for Fabrication of Thin Layer Electrode and Microelectrode: Glassy carbon rods (SIGRADUR® G) with 3mm outer diameter (OD) and 2 cm length, 5mm OD and 3.5 cm length, were purchased from HTW Hochtemperatur-Werkstoffe GmbH. 36 AWG copper wire for microelectrode fabrication was purchased from Mouser Electronics, Inc. Carbon fiber (11 µm diameter) for microelectrode fabrication was purchased from Goodfellow. Copper wire for TLE fabrication was purchased from Mouser Electronics, Inc. Conductive (silver particles containing conductive glue) and non-conductive epoxy glues, used for TLE and microelectrode fabrication, were purchased from MG Chemicals. Different sizes of glass tubes for TLE were purchased from Wilmad Lab Glass. Fused silica capillary tubing (150 µM inner diameter) was purchased from Agilent. Chemical resistance polyolefin heat shrink tubing was purchased from Raychem.

Instrumentation for Electrochemical Studies: Electrochemical experiments, including electrolysis, voltammetry, amperometry, and dual electrochemical experiments analyses, were conducted using TLEs and µEs. To perform these experiments, a Pine WaveDriver 200 EIS Bipotentiostat/Galvanostat was applied. Using the bi-potentiostat enabled us to conduct electrolysis (at GC) and voltammetric analysis (with µE) simultaneously, with a dual-electrode cyclic voltammetry (DECV) method, wherein the potential at the thin layer electrode was fixed while the potential at the microelectrode underwent continuous scanning throughout the electrolysis within the thin layer.

Instrumentation for Separation Analysis: HPLC-UV-MS analyses were performed on Shimadzu ultra-fast liquid chromatography (UFLC) system equipped with a PDA detector, coupled with an AB Sciex 3200 Q-Trap mass spectrometer using electrospray ionization. High-resolution mass spectrometry (HRMS) was performed on a Shimadzu Nexera XR (40-Series) UHPLC System coupled with a Shimadzu 9030 Q-TOF Mass Spectrometer using an ESI ionization source. Positive polarity was used on both the mass spectrometers. LC separations were performed on a Kromasil (100 mm length, 3 mm internal diameter, 3.5 µm particle size, 100 Å pore size, part number-MH3CLC10) column.

TLE and µE Fabrication: The TLE was fabricated by inserting an assembled glassy carbon rod with a heat shrink tube and solid copper into a quartz tube. The thin-layer is defined by the space between the glass tube and the rod. The µE was fabricated by inserting a carbon fiber into a glass capillary tube using a microscope, followed by sealing the tube and applying conductive and non-conductive glues. For dual electrolysis, the µE was placed in the defined thin-layer with heat shrink tubing.

Electrochemical Experiments: Cyclic voltammetry and electrolysis experiments were performed using a Pine WaveDriver 200 Bipotentiostat/Galvanostat. The bulk electrolysis reactions were conducted in an undivided cell containing a reticulated vitreous carbon (RVC) electrode. The typical cyclic voltammetric experiments were carried out with a glassy carbon (GC) electrode, and dual electrolysis was performed using the µE-TLE with a fixed potential for TLE and a scanning potential for the µE. The experiments were conducted under two mild acidic (pH=6) and acidic (pH=0.48) conditions.

Characterization of Electrolysis Products: For structural elucidation, the compounds were then analyzed with HPLC-UV-MS, a Shimadzu ultra-fast liquid chromatography (UFLC) system equipped with a PDA detector, coupled with an AB Sciex 3200 Q-Trap mass spectrometer using electrospray ionization.

ASSOCIATED CONTENT

Supporting Information

Additional figures illustrating details of TLE and µE fabrication, more electrochemical experiments, spectra, and chromatograms of the compounds.

AUTHOR INFORMATION

Corresponding Author

* Email: mrafiee@umkc.edu.

Author Contributions

MR, NN, and BTP contributed to designing research, performing research, fabricating and developing new electrochemical tools and experiments, analyzing data, and writing the paper. VM and WGG contributed to developing analytical techniques, analyzing data, and providing feedback on research design and manuscript writing.

Funding Sources

This work was supported by the School of Science and Engineering, University of Missouri-Kansas City, Kansas City of Missouri–Kansas City (UMKC).

DEDICATION

We dedicate this work to the memory of Fred C. Anson (1933–2024), a pioneer in electrochemistry and a leading contributor to the development of thin-layer electrochemistry.[28]

REFERENCES

(1) Fasan, R. Tuning P450 enzymes as oxidation catalysts. *ACS Catal.* **2012**, *2*, 647–666.

(2) Park, B. K.; Boobis, A.; Clarke, S.; Goldring, C. E. P.; Jones, D.; Kenna, J. G.; Lambert, C.; Laverty, H. G.; Naisbitt, D. J.; Nelson, S.; Nicoll-Griffith, D. A.; Obach, R. S.; Routledge, P.; Smith, D. A.; Tweedie, D. J.; Vermeulen, N.; Williams, D. P.; Wilson, I. D.; Baillie, T. A. Managing the challenge of chemically reactive metabolites in drug development. *Nat. Rev. Drug Discov.* **2011**, *10*, 292–306.

(3) Nebert, D. W.; Dalton, T. P. The role of cytochrome P450 enzymes in endogenous signalling pathways and environmental carcinogenesis. *Nat. Rev. Cancer* **2006**, *6*, 947–960.

(4) Sono, M.; Roach, M. P.; Coulter, E. D.; Dawson, J. H. Heme-containing oxygenases. *Chem. Rev.* **1996**, *96*, 2841–2888.

(5) Meunier, B.; de Visser, S. P.; Shaik, S. Mechanism of oxidation reactions catalyzed by cytochrome P450 enzymes. *Chem. Rev.* **2004**, *104*, 3947–3980.

(6) Cheng, L.; Wang, H.; Cai, H.; Zhang, J.; Gong, X.; Han, W. Iron-catalyzed arene C − H hydroxylation. *Science* **2024**, *81*, 77–81.

(7) Chambers, R. K.; Weaver, J. D.; Kim, J.; Hoar, J. L.; Krska, S. W.; Christina White, M. A preparative small-molecule mimic of liver CYP450 enzymes in the aliphatic C–H oxidation of carbocyclic N-heterocycles. *Proc. Natl. Acad. Sci. U.S.A* **2023**, *120*, 1–11.

(8) Oláh, J.; Mulholland, A. J.; Harvey, J. N. Understanding the determinants of selectivity in drug metabolism through modeling of dextromethorphan oxidation by cytochrome P450. *Proc. Natl. Acad. Sci. U.S.A.* **2011**, *108*, 6050–6055.

(9) Clardy, J.; Walsh, C. Lessons from natural molecules. *Nature* **2004**, *432*, 829–837.

(10) Guo, Y.; Lu, P.; Farrell, E.; Zhang, X.; Weller, P.; Monshouwer, M.; Wang, J.; Liao, G.; Zhang, Z.; Hu, S.; Allard, J.; Shafer, S.; Usuka, J.; Peltz, G. In silico and in vitro pharmacogenetic analysis in mice. *Proc. Natl. Acad. Sci. U.S.A.* **2007**, *104*, 17735–17740.

(11) Olsen, L. R.; Grillo, M. P.; Skonberg, C. Constituents in Kava extracts potentially involved in hepatotoxicity: A review. *Chem. Res. Toxicol.* **2011**, *24*, 992–1002.

(12) Bloom, J. D.; Labthavikul, S. T.; Otey, C. R.; Arnold, F. H. Protein stability promotes evolvability. *Proc. Natl. Acad. Sci. U.S.A.* **2006**, *103*, 5869–5874.

(13) Kim, M. J.; Kim, H.; Cha, I. J.; Park, J. S.; Shon, J. H.; Liu, K. H.; Shin, J. G. High-throughput screening of inhibitory potential of nine cytochrome P450 enzymes in vitro using liquid chromatography/tandem mass spectrometry. *Rapid Commun. Mass Spectrom.* **2005**, *19*, 2651–2658.

(14) Shanu-Wilson, J.; Coe, S.; Evans, L.; Steele, J.; Wrigley, S. Small molecule drug metabolite synthesis and identification: why, when and how? *Drug Discov. Today* **2024**, *29*, 103943.

(15) Asra, R.; Jones, A. M. Green electrosynthesis of drug metabolites. *Toxicol. Res.* **2023**, *12*, 150–177.

(16) Bussy, U.; Boujtita, M. Advances in the electrochemical simulation of oxidation reactions mediated by cytochrome P450. *Chem. Res. Toxicol.* **2014**, *27*, 1652–1668.

(17) Stalder, R.; Roth, G. P. Preparative microfluidic electrosynthesis of drug metabolites. *ACS Med. Chem. Lett.* **2013**, *4*, 1119–1123.

(18) Nikzad, N.; Rafiee, M. Electrochemical study of drug metabolism. *Curr. Opin. Electrochem.* **2024**, *44*, 101446.

(19) Rafiee, M.; Abrams, D. J.; Cardinale, L.; Goss, Z.; Romero-Arenas, A.; Stahl, S. S. Cyclic voltammetry and chronoamperometry: mechanistic tools for organic electrosynthesis. *Chem. Soc. Rev.* **2024**, *53*, 566–585.

(20) Elgrishi, N.; Rountree, K. J.; McCarthy, B. D.; Rountree, E. S.; Eisenhart, T. T.; Dempsey, J. L. A practical beginner's guide to cyclic voltammetry. *J. Chem. Educ.* **2018**, *95*, 197–206.

(21) Costentin, C.; Savéant, J. M. Concepts and tools for mechanism and selectivity analysis in synthetic organic electrochemistry. *Proc. Natl. Acad. Sci. U.S.A.* **2019**, *166*, 11147–11152.

(22) Alden, J. A., Compton, R. A. Peer Reviewed: Voltammetry—Spanning the Kinetic Timescale. *Anal. Chem.* **2000**, *72*, 198–203.

(23) Van Den Brink, F. T. G.; Büter, L.; Odijk, M.; Olthuis, W.; Karst, U.; Van Den Berg, A. Mass spectrometric detection of short-lived drug metabolites generated in an electrochemical microfluidic chip. *Anal. Chem.* **2015**, *87*, 1527–1535.

(24) Sandford, C.; Edwards, M. A.; Klunder, K. J.; Hickey, D. P.; Li, M.; Barman, K.; Sigman, M. S.; White, H. S.; Minteer, S. D. A synthetic chemist's guide to electroanalytical tools for studying reaction mechanisms. *Chem. Sci.* **2019**, *10*, 6404–6422.

(25) Shin, S. J.; Kim, J. Y.; An, S.; Chung, T. D. Recent advances in electroanalytical methods for electroorganic synthesis. *Curr. Opin. Electrochem.* **2022**, *35*, 101054.

(26) Wasalathanthri, D. P.; Mani, V.; Tang, C. K.; Rusling, J. F. Microfluidic electrochemical array for detection of reactive metabolites formed by cytochrome P450 enzymes. *Anal. Chem.* **2011**, *83*, 9499–9506.

(27) Punchihewa, B. T.; Minda, V.; Gutheil, W. G.; Rafiee, M. Electrosynthesis and microanalysis in thin Layer: an electrochemical pipette for rapid electrolysis and mechanistic study of electrochemical reactions. *Angew. Chem. Int. Ed.* **2023**, *62*, e202312048.

(28) Christensen, C. R.; Anson, F. C. Chronopotentiometry in thin layers of solution. *Anal. Chem.* **1963**, *35*, 205–209.

(29) Bard, A. J.; and Faulkner, L. R. *Electrochemical methods: fundamentals and applications*. (John Wiley & Sons, 2000), pp.163

(30) Yildiz, A.; Kissinger, P. T.; Reilley, C. N. Evaluation of an improved thin-layer electrode. *Anal. Chem.* **1968**, *40*, 1018–1024.

(31) Sheaffer, J. C.; Peters, D. G. Simple electrode for thin-layer electrochemistry. *Anal. Chem.* **1970**, *42*, 430–432.

(32) Hubbard, A. T.; Peters D. G. Electrochemistry in thin layers of solution. *Crit. Rev. Anal. Chem.* **1973**, *3*, 201-242.

(33) Shin, S. J.; Kim, J. Y.; An, S.; Kim, M.; Seo, M.; Go, S. Y.; Chung, H.; Lee, M. K.; Kim, M. G.; Lee, H. G.; Chung, T. D. Revisiting thin-layer electrochemistry in a chip-type cell for the study of electro-organic reactions. *Anal. Chem.* **2022**, *94*, 1248–1255.

(34) Punchihewa, B. T.; Khalafi, L; Rafiee, M. Electrolysis in thin layer: A technique for electroanalytical and electrosynthetic applications. *Curr. Opin. Electrochem.* **2024**, *44*, 101445.

(35) https://www.youtube.com/shorts/tHjEWD3Y-OA, accessed October 9, 2024.

(36) https://www.youtube.com/shorts/S17xPxQo24A, accessed October 9, 2024.

(37) Engstrom, R. C.; Weber, M.; Wunder, D. J.; Burgess, R.; Winquist, S. Measurements within the diffusion layer using a microelectrode probe. *Anal. Chem.* **1986**, *58*, 844–848.

(38) Klopčič, I.; Dolenc, M. S. Chemicals and drugs forming reactive quinone and quinone imine metabolites. *Chem. Res. Toxicol.* **2019**, *32*, 1–34.

(39) Nematollahi, D.; Shayani-Jam, H.; Alimoradi, M.; Niroomand, S. Electrochemical oxidation of Acetaminophen in aqueous solutions: Kinetic evaluation of hydrolysis, hydroxylation and dimerization processes. *Electrochim. Acta* **2009**, *54*, 7407–7415.

(40) Bender, R. P.; Lindsey, R. H.; Burden, D. A.; Osheroff, N. N-Acetyl-p-benzoquinone imine, the toxic metabolite of Acetaminophen, is a topoisomerase II poison. *Biochemistry* **2004**, *43*, 3731–3739.

(41) Saikrithika, S.; Senthil Kumar, A. In Situ Electrochemical trapping and unraveling the mechanism of the toxic intermediate metabolite N-Acetyl- p-Benzoquinone imine of the Acetaminophen drug and its biomimetic mediated NADH oxidation reaction. *J. Phys. Chem. C* **2023**, *127*, 8016–8029.

(42) Bussy, U.; Delaforge, M.; El-Bekkali, C.; Ferchaud-Roucher, V.; Krempf, M.; Tea, I.; Galland, N.; Jacquemin, D.; Boujtita, M. Acebutolol and alprenolol metabolism predictions: Comparative study of electrochemical and cytochrome P450-catalyzed reactions using liquid chromatography coupled to high-resolution mass spectrometry. *Anal. Bioanal. Chem.* **2013**, *405*, 6077–6085.

(43) Bussy, U.; Ferchaud-Roucher, V.; Tea, I.; Krempf, M.; Silvestre, V.; Boujtita, M. Electrochemical oxidation behavior of Acebutolol and identification of intermediate species by liquid chromatography and mass spectrometry. *Electrochim. Acta* **2012**, *69*, 351–357.

(44) Rollins, D. E.; Von Bahr, C.; Glaumann, H.; Moldéus, P.; Rane, A. Acetaminophen: Potentially toxic metabolite formed by human fetal

and adult liver microsomes and isolated fetal liver cells, *Science* **1979**, *205*, 1414–1416.

(45) The voltammetric current of the products after the electrolysis reaction was used to quantify the amount of electrochemically generated quinone imine, assuming the same diffusion coefficient for the redox partners (i.e. 2d and 2c). The identity of these products was confirmed based on their peak potential and verified by high-resolution mass spectroscopy (please see sections 6 and 7 in Supporting Information). Quantification of quinone imine 2c via HPLC-MS was not possible due to its retention time and low stability. However, semiquantitative analysis of HPLC-MS intensity (by comparing peak ratios) indicates that the intensity of the 2c peak in TLE is more than 18 times greater than that in the traditional electrolysis setup.

(46) Baillie, T. A. Metabolism and toxicity of drugs. Two decades of progress in industrial drug metabolism. *Chem. Res. Toxicol.* **2008**, *21*, 129–137.

(47) Johansson, T.; Jurva, U.; Grönberg, G.; Weidolf, L.; Masimirembwa, C. Novel metabolites of amodiaquine formed by CYP1A1 and CYP1B1: Structure elucidation using electrochemistry, mass spectrometry, and NMR. *Drug Metab. Dispos.* **2009**, *37*, 571–579.

(48) The video in this link demonstrates a screen recording of an animated presentation showcasing the progression and sequence of simultaneous electrochemical experiments: https://www.youtube.com/shorts/ajg6JSPkRvw, accessed October 9, 2024.

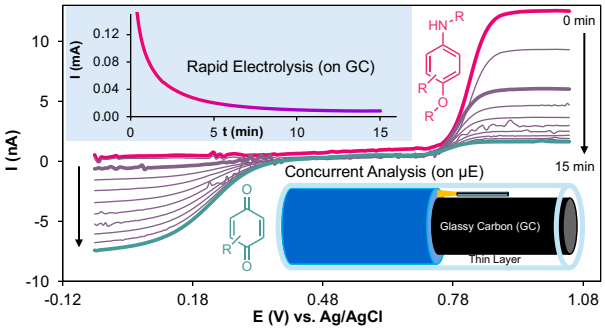

TOC